energies

MDPI

Review

Cobalt-Based Electrolytes for Dye-Sensitized Solar Cells: Recent Advances towards Stable Devices

Federico Bella [1,*], Simone Galliano [2], Claudio Gerbaldi [1] and Guido Viscardi [2]

[1] GAME Lab, CHENERGY Group, Department of Applied Science and Technology—DISAT, Politecnico di Torino, Corso Duca degli Abruzzi 24, 10129 Torino, Italy; claudio.gerbaldi@polito.it

[2] Department of Chemistry and NIS Interdepartmental Centre, Università degli Studi di Torino, Via Pietro Giuria 7, 10125 Torino, Italy; simone.galliano@unito.it (S.G.); guido.viscardi@unito.it (G.V.)

* Correspondence: federico.bella@polito.it; Tel.: +39-011-090-3448

Academic Editor: Tapas Mallick

Received: 10 April 2016; Accepted: 11 May 2016; Published: 19 May 2016

Abstract: Redox mediators based on cobalt complexes allowed dye-sensitized solar cells (DSCs) to achieve efficiencies exceeding 14%, thus challenging the emerging class of perovskite solar cells. Unfortunately, cobalt-based electrolytes demonstrate much lower long-term stability trends if compared to the traditional iodide/triiodide redox couple. In view of the large-scale commercialization of cobalt-based DSCs, the scientific community has recently proposed various approaches and materials to increase the stability of these devices, which comprise gelling agents, crosslinked polymeric matrices and mixtures of solvents (including water). This review summarizes the most significant advances recently focused towards this direction, also suggesting some intriguing way to fabricate third-generation cobalt-based photoelectrochemical devices stable over time.

Keywords: dye-sensitized solar cell; cobalt electrolyte; cobalt complex; stability; polymer electrolyte; quasi-solid electrolyte

1. Introduction

Dye-sensitized solar cells (DSCs) have recently exceeded 14% efficiency values [1] and are day by day establishing themselves as the leading photovoltaic technology in the fields of building-integrated and indoor light-harvesting [2–6]. In these devices, the electrolyte plays a central role in determining both efficiency and durability [7,8]. Indeed, the redox couple dissolved in the organic solvent has the aim of capturing electrons that reach the counter-electrode [9–11] and to regenerate the oxidized dye acting as a sensitizer [12–14].

Since their discovery in 1991 [15,16], the redox mediator at the base of the DSC operation has been the iodide/triiodide couple (I^-/I_3^-). Indeed, it presents fast sensitizer regeneration kinetics and a slow recombination reaction with the electrons in the TiO_2 conduction band. However, the iodine-based redox shuttle possesses a number of unfavorable characteristics [17]. Indeed, its redox potential (+0.11 V *vs.* SSCE, SSCE = saturated salt calomel electrode) is not ideally positioned for many sensitizers [18–20], leading to a significant loss in the maximum open circuit potential (V_{oc}) and a corresponding loss in the maximum overall power conversion efficiency (PCE) of the cells. Furthermore, I_3^- and other polyiodides present in the electrolyte absorb a good portion of visible light (300–450 nm), thus leading to lower short-circuit photocurrent density (J_{sc}) values due to the subtraction of photons to the photoactive dye molecules. When upscaling of DSCs is conceived of, it must also be considered that the iodine-based redox couple corrodes copper/silver lines used to collect the electrons in large-scale modules.

Among the different redox couples proposed in the last two decades to replace the iodine-based one, cobalt complexes are particularly promising mediator alternatives for several reasons [21].

They are generally less colored than iodine solutions and therefore compete less with the dye in visible light absorption. Moreover, cobalt complexes are noncorrosive to metal cathodes and non-volatile. Recently, the chemical community worked intensively on these redox mediators because they have synthetically-tunable redox potentials [22–25], which makes them particularly promising to identify structure/property relationships. In fact, the DSC community is interested in having a library of available cobalt complexes with tuned redox potentials that can be coupled with dyes and semiconductors purposely chosen for the final destination of the device. Moreover, cobalt-based redox shuttle mediators generally show more positive redox potentials than I^-/I_3^-, therefore resulting particularly interesting in maximizing the V_{oc} of DSCs.

As stated above, the stability of DSCs is a critical aspect for their commercialization [26–29]. Indeed, a minimum of 1000 h of continuous illumination at one sun (100 mW cm^{-2}, AM 1.5G) represents a common benchmark [28] for proposing stable cells. This aging period is roughly equivalent, in absorbed photons, to one year of outdoor exposure at the optimum tilt in London and to about six months in an arid location in Spain or the USA. While stability studies have been extensively detailed in the literature for the traditional iodine-based redox couple, it is rather surprising that only very few works detail the aging of cobalt-based DSCs, which is often performed for less than 500 h and rarely under photochemical or thermal stress. Based on such a scenario, the scientific community started considering the cobalt-based redox couples as unstable, as also suggested by the fact that none of the recent records obtained (up to 14.3% [1]) in the presence of cobalt-based electrolytes have ever been certified. In fact, the reader can check the table from the National Center for Photovoltaics (NCPV) by the National Renewable Energy Laboratory (NREL) [30], finding that the certified record efficiency for DSCs is still 11.9% (2012) by Sharp, obtained with iodine-based electrolytes.

As a result, the stability of cobalt-based cells has become a matter of intense study by the scientific community over the past five years. In this review, we propose some of the strategies described in the literature to improve the stability of these solar cells. In the first part of the work, we show that the chemical structure of the cobalt complex can be tailored to increase its photostability and compatibility with the photoanode, also choosing suitable additives. Subsequently, it is proposed that the volatility of the organic solvents-based electrolytes may be limited through the introduction of ionic liquids, inorganic nanoparticles or polymeric matrices. Finally, we propose a recent and emerging trend in the field of DSCs, focused on the development of totally aqueous electrolytes (non-flammable and less volatile than acetonitrile (ACN)-based ones), where cobalt complexes show an excellent synergy in terms of solubility, efficiency and stability.

2. Liquid Electrolytes: Tuning of Cobalt Complexes' Chemical Structure and Finding Suitable Additives to Increase Stability

In this section, we propose liquid electrolytes containing cobalt complexes, the stability of which was investigated by photochemical and/or thermal aging tests. The variation of the chemical structure of the complexes, the presence of specific additives in the electrolytes and the replacement of organic solvents with ionic liquids are the three strategies proposed in the literature to improve the stability of these liquid DSCs.

The combination between high redox potential and stability of the mediators is one of the fundamental aspects to be taken into account when formulating new cobalt complexes. Indeed, a smart strategy to achieve high V_{oc} values is represented by the use of ligands with multiple electron-withdrawing groups that positively shift the redox potentials of the resulting complexes. However, it should be reminded here that ligands with strong electron withdrawing groups can lead to lower complex stability. This is ascribable to the loss of electron density from the lone pair on the bipyridine (bpy) nitrogen atoms, which makes the ligand a weaker and more labile σ-donor (Lewis base). On the other hand, electron-withdrawing groups could also make ligands stronger π-acceptors, thus leading to an overall unpredictable effect on the complex stability.

For this purpose, Kirner *et al.* [31] firstly prepared and characterized three promising cobalt complexes and determined the approximate stability constants by a newly-proposed NMR experiment. Indeed, the NMR quantification of free, dissociated ligands is a rapid experiment to directly determine an approximate stability constant. $[Co(dma\text{-}bpy)_3]^{2+}$ (dma-bpy = 2,2′-bipyridine-4,4′-bis(N,N-dimethylcarboxamide)), $[Co(me\text{-}bpy)_3]^{2+}$ (me-bpy = 2,2′-bipyridine-4,4′-bis(methyl ester)) and $[Co(cn\text{-}bpy)_3]^{2+}$ (cn-bpy = 2,2′-bipyridine-4,4′-dicarbonitrile) were proposed as novel complexes combined with Z907 [*cis*-bis(isothiocyanato)(2,2′-bipyridyl-4,4′-dicarboxylato)(4,4′-di-nonyl-2′-bipyridyl)ruthenium(II)] as the sensitizer. Experiments carried out by Kirner *et al.* highlighted several interesting aspects: (i) the appearance of multiple waves in the cyclic voltammetry; (ii) a color change upon the addition of 4-*tert*-butylpyridine (TBP), indicating the formation of a new species; (iii) the direct NMR evidence of free dissociated ligand in the ACN solution; (iv) the potential-independent DSC recombination currents paralleling the stability trends as determined by NMR. Overall, these observations revealed a trend of decreasing the complex stability with increasing the redox potential. In particular, the instability of $[Co(me\text{-}bpy)_3](ClO_4)_2$ and $[Co(cn\text{-}bpy)_3](ClO_4)_2$ complexes render them underprivileged choices as mediators in DSCs; moreover, they were found to be poorly soluble in organic solvents. On the other hand, $[Co(dma\text{-}bpy)_3](ClO_4)_2$ showed superior stability. Kirner *et al.* concluded their work stating that designing ligand structures alternative to bipyridine (e.g., phenanthroline, terpyridine, clathrochelate) should be considered as a primary strategy towards stable cobalt complexes. However, to date, no demonstration of the long-term stability of these newly-proposed molecules has been reported.

The type and number of donor atoms (denticity) that ligands use to form the cobalt coordination sphere is of paramount importance. Indeed, a high denticity usually results in a high overall stability constant of the complex through the chelating effect [32]. Moreover, the denticity of the ligands affects the reorganization energies associated with electron transfer processes involving the $Co^{2+/3+}$ redox states [33], thus influencing the rates of important charge-transfer steps, such as charge recombination and dye regeneration. In order to develop a redox shuttle based on complexes with very high thermodynamic stability, Kashif *et al.* proposed a cobalt complex of hexapyridyl ligand (6,6′-bis(1,1-di(pyridin-2-yl)ethyl)-2,2′-bipyridine, bpyPY4) as the redox mediator, also comparing its photovoltaic performance and stability to the reference shuttle $[Co(bpy)_3]^{2+/3+}$ with trifluoromethanesulfonate ($CF_3SO_3^-$) as the counterion [34]. $[Co(bpyPY4)](CF_3SO_3)_2$ (namely 1a, Figure 1A) and $[Co(bpyPY4)]\text{-}(CF_3SO_3)_3$ (namely 1b, Figure 1B) were introduced in ACN at concentrations of 0.20 and 0.10 M, respectively, together with bis(trifluoromethane)sulfonimide lithium salt (LiTFSI) 50 mM and 1-methylbenzimidazole (NMBI) 0.50 M. An impressive efficiency of 8.3% was achieved for the resulting DSC, while a PCE equal to 7.8% was measured for the standard MK2/$[Co(bpy)_3]^{2+/3+}$ electrolyte combination, where MK2 is 2-cyano-3-[5‴-(9-ethyl-9*H*-carbazol-3-yl)-3′,3″,3‴,4-tetra-*n*-hexyl-[2,2′,5′,2″,5″,2‴]-quater thiophen-5-yl] acrylic acid. This was likely due to the lower electrochemical driving force for dye regeneration in the case of $[Co(bpy)_3]^{2+/3+}$ (340 mV) compared to 1a/1b (435 mV). Furthermore, light soaking experiments of the devices sensitized with 1a/1b for 20 min under one sun irradiation resulted in a further increase in J_{sc} and a slight decrease in V_{oc}, giving rise to an overall PCE of 9.4%.

The evolution of the DSC performance for devices based on 1a/1b and $[Co(bpy)_3]^{2+/3+}$ redox mediators was also studied by Kashif *et al*. DSCs were tested under continuous full sunlight intensity at 45% humidity and 25–30 °C over a period of 100 h (Figure 1C). The authors also studied the effect of two different Lewis base additives: *p*-trifluoromethylpyridine (TFMP), a comparatively milder Lewis base, and NMBI. However, the addition of TFMP to $[Co(bpy)_3]^{2+/3+}$ led to a green precipitate, and the resulting devices showed very poor stability; in contrast, no precipitation was observed in the 1a/1b/TFMP electrolytes, and DSCs gave comparable efficiencies to the 1a/1b/NMBI electrolyte system. DSCs based on electrolyte 1a/1b clearly outperformed those assembled with the reference mediator $[Co(bpy)_3]^{2+/3+}$, showing a >20% performance increase over the first 24 h of continuous illumination. Moreover, when TFMP was used, DSCs based on 1a/1b initially showed a 20% increase in

performance, which was maintained across the full 100-h testing period. Such an effect was attributed to the excellent thermal, hydrolytic and oxidative stability of fluorinated aromatic hydrocarbons, such as TFMP [35].

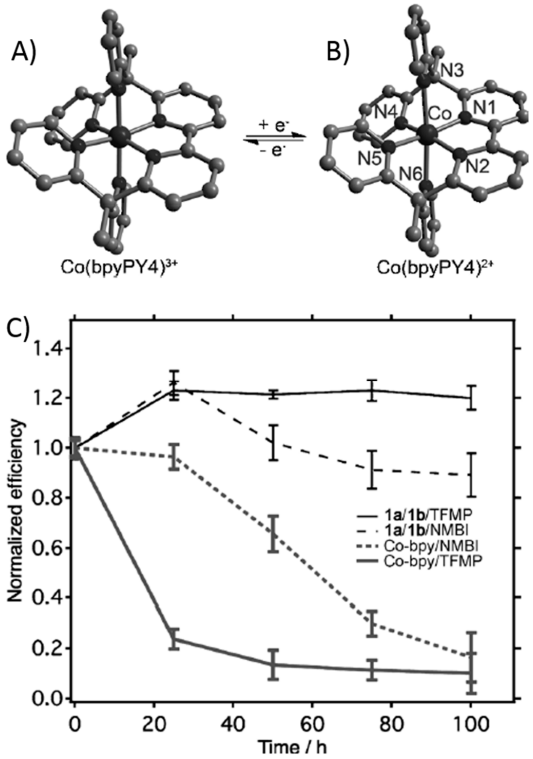

Figure 1. Molecular structures of $[Co\text{-}(bpyPY_4)]^{2+/3+}$ in crystals of 1a (**A**) and 1b (**B**). (**C**) Normalized efficiencies of the devices under the aging experiment at full sunlight intensity with a 400-nm UV cut-off filter. Two Lewis bases, NMBI and TFMP, were alternatively used with 1a/1b and $[Co(bpy)_3]^{2+/3+}$. Adapted and reprinted with permission from [34].

Besides focusing on the chemical structure of cobalt complexes, their interactions with dye molecules deserve attention, DSC being a device strongly influenced by interfaces. For this purpose, Mosconi *et al.* published a combined experimental and computational investigation to understand the nature of the interactions between cobalt redox mediators and TiO_2 surfaces (sensitized by ruthenium or organic dyes) [36]. Both N719- and Z907-based DSCs (*i.e.*, sensitized with ruthenium dyes) showed an increased lifetime in iodine-based electrolyte compared to the cobalt-based redox shuttle, while the organic (E)-3-(5-(5-(4-(bis(4-(hexyloxy)phenyl)thiophene-2-yl)thiophene-2-yl)-2-cyanoacrylic acid (D21L6) and (E)-3-(5-(5-(4-(bis(4-(dodecyloxy)phenyl)thiophene-2-yl)thiophene-2-yl)-2-cyanoacrylic acid (D25L6) dyes, endowed with long alkoxy chains, showed no significant change in the electron lifetime regardless of the employed electrolyte. *Ab initio* molecular dynamics simulations showed the formation of a complex between the cobalt electrolyte and the surface-adsorbed ruthenium dye, which brought the $[Co(bpy)_3]^{3+}$ species into contact with the TiO_2 surface. This led to a high probability of intercepting TiO_2-injected electrons by the oxidized $[Co(bpy)_3]^{3+}$ species, lying close to the N719-sensitized TiO_2 surface, where N719 is di-tetrabutylammonium *cis*-bis(isothiocyanato)bis(2,2′-bipyridyl-4,4′-dicarboxylato)ruthenium(II).

DSCs are multi-component devices [37–40], and there are inevitably various factors influencing their efficiency and stability [41–43]; one decisive factor is the electrolyte, composed of the redox shuttles, a selection of additives and a solvent (or a mixture of solvents). In particular, additives such as lithium salts and TBP were proven to be highly necessary for achieving high performance. Indeed, Li^+ ions are expected to cause a lowering of the TiO_2 conduction band energy level,

thus leading to an improvement in electron injection efficiency and electron lifetime [44]; on the contrary, TBP typically gives a negative shift of the TiO_2 conduction band, and reduced interfacial recombination losses are observed, resulting in a relatively higher V_{oc} [45]. It is quite surprising to find only very few papers addressing the influence of these additives on the durability of cobalt-based DSCs, despite an extensive literature being found for the iodide/triiodide redox mediator [46–49], also taking into account the role of different counterions [50,51]. Only recently, Gao *et al.* have reported that higher concentrations of the cobalt-based redox components, in both the reduced and, surprisingly, the oxidized forms, offer improved long-term stability with the limited drawback of a lower initial PCE [52]. In order to deeply study the concentration-dependent influence and the effect of some additives on the device stability, the authors developed a series of electrolytes containing higher concentrations of $Co(bpy)_3^{2+}$ and $Co(bpy)_3^{3+}$ and bearing the tetracyanoborate counterion in ACN; these electrolytes were compared to a standard liquid electrolyte (with a 0.22/0.05 molar ratio between reduced and oxidized species) in D35-sensitized cells (D35 = (E)-3-(5-(4-(bis(2',4'-dibutoxy-[1,1'-biphenyl]-4-yl)amino)phenyl)thiophen-2-yl)-2-cyanoacrylic acid). A stability test lasting 1000 h was carried out under strong light soaking conditions (one sun illumination and 60 °C). Measurements by Gao *et al.* demonstrated a significant correlation between device stability and cobalt complex concentration, and the best values were obtained for the electrolyte named AN-Hi-L (0.30/0.15 molar ratio between reduced and oxidized species). This outcome was also confirmed by electrochemical impedance spectroscopy (EIS) investigation, which showed that cells containing lower concentrations of the redox couple suffered from more serious mass-transport limitation and lower electron lifetime after the long-term light soaking experiment.

Gao *et al.* also evaluated the effect of additives. In particular, the addition of lithium salt (*i.e.*, $LiClO_4$ 0.10 M) increased the initial PCE, but rather unexpectedly, a worse long-term stability was observed in comparison to the device filled with Li^+-free electrolytes (namely, AN-HI), probably due to an increase in the interfacial charge recombination during the ageing test (Figure 2). Interestingly, the AN-HI electrolyte-based cell showed a 4% enhanced PCE after 1000 h as compared to the initial value. As regards the addition of TBP in the electrolytes, different concentrations ranging from 0 to 0.70 M were explored, and it was observed that all of the four photovoltaic parameters considerably increased by adding up to 0.20 M of TBP. On the other hand, the increase of the TBP concentration led to a rapid decline of both V_{oc} and J_{sc} and, consequently, PCE. These results clearly indicate the two side effects of TBP on cobalt-based DSC devices: initially, it suppresses the interfacial recombination well, as commonly reported in the literature, but during the stability test, a higher concentration of TBP induces a faster increase in the recombination loss, in good agreement with the observed faster V_{oc} lowering. The proposed reason for its adverse impact is that TBP is a relatively strong Lewis base and can induce dye desorption. Therefore, a change in the surface structure is caused, resulting in an enhancement of the recombination losses; reasonably, this effect may be accelerated by the light soaking experiment.

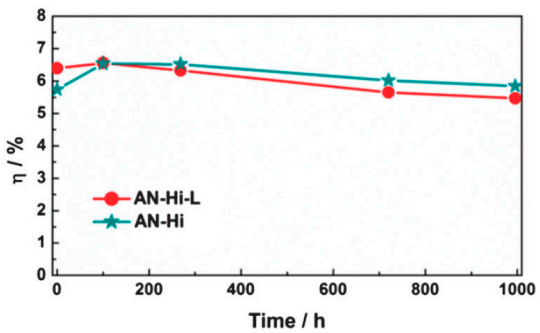

Figure 2. Efficiency variation over time for DSCs based on the electrolytes AN-Hi-L and AN-Hi during the stability test. Adapted and reprinted with permission from [52].

Since photostability has been identified as one of the main limiting factors of cobalt-based DSCs, O'Regan *et al.* performed a 2000-h photostability test of these cells [53]. In their investigation, two different electrolytes were used: "ACN", acetonitrile with $[Co(bpy)_3](PF_6)_2$ 0.20 M, $Co[(bpy)_3](PF_6)_3$ 40 mM, TBP 0.50 M and $LiClO_4$ 0.10 M, and "MPN", 3-methoxypropionitrile with $Co[(bpy)_3](PF_6)_2$ 0.20 M, $Co[(bpy)_3](PF_6)_3$ 0.10 M, TBP 0.50 M and $LiClO_4$ 0.10 M. Measuring the stability of the electrolyte was the purpose of the work; thus, a standard ruthenium sensitizer (Z907) was selected due its well-known long-term stability. Of course, Z907 cannot be as efficient as porphyrin sensitizers in the presence of a cobalt-based redox shuttle, but the use of organic dyes would have added an additional instability.

The light soaking experiment by O'Regan *et al.* [53] was carried out under one sun irradiation, provided by white LEDs, at 20 °C and at the V_{oc}. After 2000 h, the efficiency of the ACN cells decreased by 34% and the PCE of the MPN cell decreased by 10%. Overall, an early decrease in the fill-factor (FF) mostly accounted for the decrease in overall efficiency, followed, in the ACN cells, by a slow decline in the photocurrent. On the other hand, V_{oc} was completely stable for all of the cells. More in detail (as shown in Figure 3), a rapid increase in the photocurrent occurred in the initial phase of the experiment, accompanied by an increase in the series resistance. Photocurrent stabilized 200 h later, when also a slow degradation of FF was observed. By further investigations, it was shown that the diffusion resistance of the electrolyte (R_d) increased continuously through the experiment, in correlation with the FF of the cells over time. Such a strong correlation indicated that changes in the electrolyte were connected to the degradation in the FF observed under illumination. Recombination phenomena at the photoanode/electrolyte interface were excluded, since the charge transfer resistance (R_{ct}) increased steadily during illumination, thus leading to a decreased recombination rate constant over time.

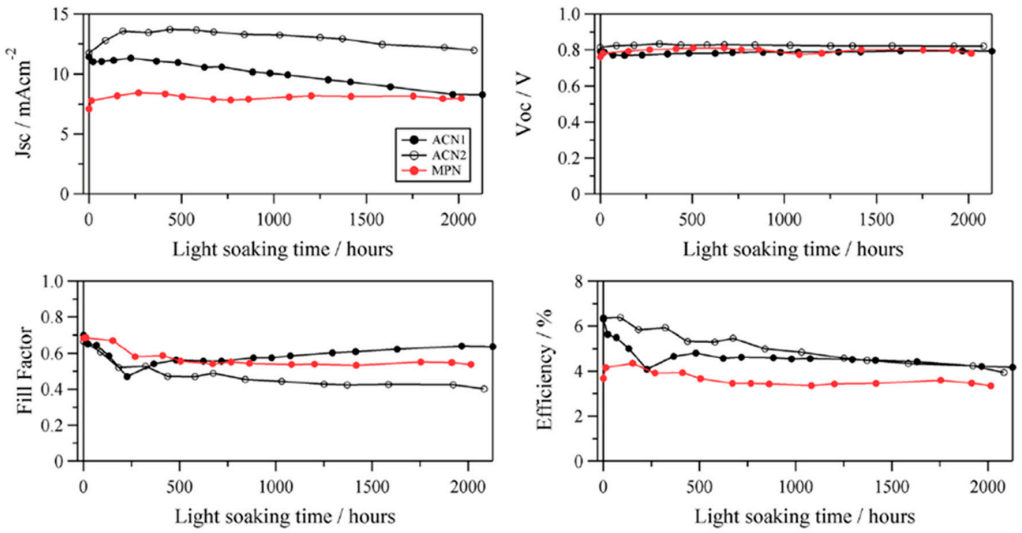

Figure 3. Performance parameters of cells subjected to 2000 h of continuous light soaking at one sun equivalent (LED illumination) and 20 °C. Adapted and reprinted with permission from [53].

The measured increase in the diffusion resistance could be attributed to a decrease in the concentration of the ions, an increase in the electrolyte viscosity or a blockage of the porosity of the photoelectrode. By examining several concentrations of the redox mediator, O'Regan *et al.* found that the trend of FF values was caused by a degradation in the ability of the Co(III) species to diffuse out of the pores. As a consequence, increased recombination losses were measured. In addition, photochemical ligand replacement on the cobalt and development of electrolyte concentration gradients laterally across the cell were hypothesized, but not verified.

In the eternal debate on the role of additives in liquid electrolyte-based DSCs, a truly original investigation was carried out by Gao *et al.*, who studied the effects of several salts (imidazolium-

and ammonium-based) that, from a size and polarizing power perspective, represented intermediate Lewis acidity between electrolytes containing Li^+ and those containing no cation co-additive at all [54]. The authors measured the photovoltaic performance of fresh DSCs in the absence (cation-free, in the sense of added salts) and presence of different cation co-additives including standard Li^+ salts and other monovalent cations with the same anion, but exhibiting a lower Lewis acidity and a lower charge-to-size ratio: 1-ethyl-3-methylimidazolium (EIm^+), tetraethylammonium (TEA^+), 1-butyl-3-methylimidazolium (BIm^+) and tetrabutyl cation (TBA^+). The J_{sc} of these devices showed a clear cation dependency of $Li^+ > EIm^+ >$ cation-free, while the presence of other organic cations gave results similar to the cation-free cells. Such a difference in the photocurrent can be interpreted as indicating a cation-specific ability to tune the TiO_2 surface charge and energy levels, thus influencing the electron injection efficiency of the sensitizer.

A 1000-h accelerated aging under sunlight was performed by Gao *et al.* (see Figure 4A,B) [54], while tests under dark conditions were simultaneously conducted to assess the photostability of these devices. Results for the BIm^+-, TEA^+- and TBA^+-containing DSCs were similar to those of the cation-free cells. In these devices, upon early exposure to light, a boost in J_{sc} was observed. In the long term, exposure to light was the main cause of the overall decrease in both PCE and FF. The decline in V_{oc} also showed a light-induced difference, being faster than that under heat alone. The photoinstability of all of these parameters strongly depended on the cation co-additive in the electrolyte: cation-free < EIm^+ < Li^+. The J_{sc} enhancement observed for the Li^+-free cells after a short-term exposure to full solar irradiation was particularly surprising, and it was attributed to a better electron injection efficiency and to a Stark effect. This latter reflected the absorption perturbation of anchored dyes and was noted as a bleach at *ca.* 550 nm for the D35 dye, caused by the change in the adjacent electric field. It is well known that the electric field over the dye molecules, which mainly determines the bleach intensity, is generated by the injected electrons upon light illumination and the adjacent polarizing electrolyte cations. In the system studied by Gao *et al.* [54], a red shift (20 to 30 nm) was found for the Stark bleach of the dye/TiO_2 films in contact with Li^+-free electrolytes in the aging test; by contrast, only a small relative change was observed in the case of the Li^+-containing electrolyte.

Figure 4B shows that a decrease in V_{oc} was strongly related to the light exposure and to the electrolyte cation co-additives. When the exposure to light was prolonged, the electron lifetime for the Li^+-containing cells continued to decrease significantly and faster than the Li^+-free cells. The authors stated that the change in dye attachment correlates with DSC stability, including both dye desorption (that may occur simply according to an adsorption/desorption thermodynamic equilibrium) and dye degradation (that may derive from the fact that photoexcited dyes are vulnerable to chemical attack under open-circuit conditions). The pronounced dye desorption is presumably caused by the addition of a Lewis base (such as TBP), but it is suppressed by co-added cations, most dramatically by Li^+ (that can induce electrolyte acidity by reducing the TBP effect by a simple Lewis base/acid coordination in the electrolyte) and the cationic cobalt complexes. The rates of dye degradation with different additives and at different aging conditions are shown in Figure 4C. On exposure to light, the dye molecules are almost depleted within 200 h in the presence of Li^+, which is much faster than in the presence of EIm^+ or on exposure to heat. Moreover, since water had previously been shown to play an important role in dye degradation [55] and considering that Li^+ salts are hygroscopic, a dehydrated Li^+ salt was employed for comparison. A difference in the early rate due to the addition of Li^+ ions was noted, but not in the total amount of dye degradation when the same amount of water was added. However, in the water-free case, Li^+ ions caused less degradation, and the process seemed to follow a different trend, demonstrating that absorbed water is not the main reason for the Li^+-induced dye degradation.

Even if the work by O'Regan *et al.* [53] demonstrated an outstanding long-term stability under light soaking, problems of evaporation and leakage arising from the use of volatile organic solvents still restrict the large-scale diffusion of DSCs. For this purpose, ionic liquids could represent a viable solution, given the fact that they are organic salts with melting points at below (or near) room

temperature and have been extensively studied as alternative electrolytes in several energy devices thanks to their low volatility, high conductivity and thermal characteristics and wide electrochemical stability window [56–60].

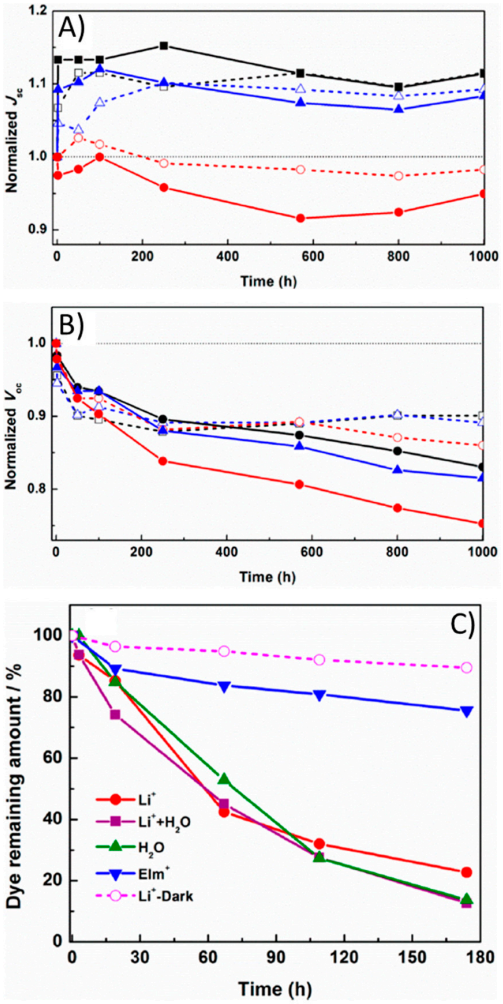

Figure 4. (**A**,**B**) Evolution of photovoltaic parameters with aging time for DSCs having different cation compositions: cation-free (■), Li^+ (●) and EIm^+ (▲) under full sun illumination (390-nm cut-off filter, solid lines) and in dark conditions (dashed lines) at a temperature of 60 °C. All data are normalized with respect to the initial value. All of the electrolytes were prepared in air according to the same recipe: $Co(bpy)_3[B(CN)_4]^{2+/3+}$ 0.30 M/0.15 M, TBP 0.20 M and 0.10 M of cation co-additives. (**C**) Degradation rates of the 20 μM D35/acetonitrile solution containing different additives: anhydrous Li^+ 5 mM, anhydrous Li^+ 5 mM + H_2O 50 mM, H_2O 50 mM, EIm^+ 5 mM, recorded with aging time on exposure to light at 60 °C; a cell laden with anhydrous Li^+ 5 mM on exposure at 60 °C is also shown. Adapted and reprinted from [52].

In 2013, Xu *et al.* reported a pioneering work proposing a promising ionic liquid consisting of an imidazolium functionalized Co(II/III) complex [61]. Since the standard cobalt complexes are scarcely soluble in ionic liquid-based electrolytes, the authors directly synthesized an ionic liquid bearing in its core structure a cobalt tris(bipyridyl) unit, namely $[Co((MeIm\text{-}bpy)PF_6)_3]^{2+/3+}$, where $(MeIm\text{-}bpy)PF_6)_3$ is the 3,3′-(2,2′-bipyridine-4,4′-diylbis(methylene))bis(1-methyl-1H-imidazol-3-ium)hexafluorohosphate) shown Figure 5A. Using N719 dye as a photosensitizer, overall PCE values of 7.37% (one sun) and 8.29% (0.5 suns) were achieved in a binary ionic liquid-based electrolyte having the following composition: $[Co((MeIm\text{-}bpy)PF_6)_3]^{2+}$ 50 mM, nitrosonium tetrafluoroborate ($NOBF_4$) 20 mM,

guanidinium thiocyanate (GuNCS) 0.14 M, TBP 0.5 M in a mixture of 1-propyl-3-methylimidazolium iodine (PMII) and 1-ethyl-3-methylimidazolium thiocyanate (EMINCS) in a 13 to 7 (V/V) ratio. Both values are considerably higher than the efficiencies of the corresponding iodine-based cells (6.39% and 6.97%, respectively) under the same irradiation conditions. The increase in performance for the cobalt-based devices was ascribed to improved J_{sc} and V_{oc}. Indeed, an enhanced photocurrent response was observed in the spectral range from 370 to 480 nm, which is ascribed to the negligible light absorption typical of cobalt complexes (Figure 5B). As regards the photovoltage, the cobalt-based mediator positively shifted the TiO_2 conduction band of 30 mV, but its Nernst potential is about 170 mV more positive than that of its iodine-based counterpart. Another reason for the higher V_{oc} measured for the cobalt system is that the attached bulky imidazole groups increase the steric hindrance of the cobalt complex, thus preventing the electron recombination loss reaction at the photoelectrode/electrolyte interface, also increasing the electron lifetime [62].

The long-term stability of the $[Co((MeIm\text{-}bpy)PF_6)_3]^{2+/3+}$-based cells was measured under prolonged irradiation. For this experiment, the cell was covered with a UV cut-off filter and irradiated under open circuit conditions at ambient temperature. The devices retained around 76% of their initial conversion efficiency after 800 h of testing. The decreased conversion efficiency of the DSCs was mainly due to the decrease of V_{oc} and FF values (Figure 5C), but the authors did not provide a justification for these effects.

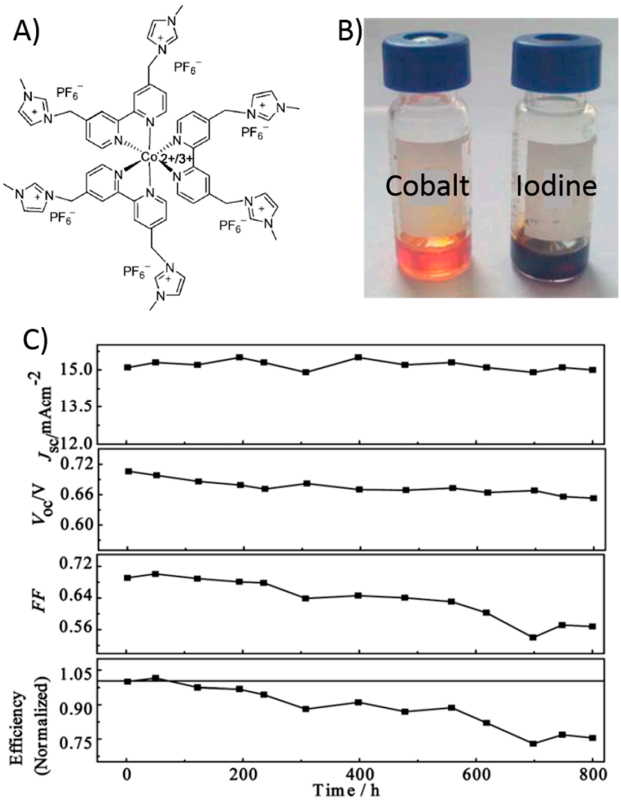

Figure 5. (**A**) Chemical structure of $Co((MeIm\text{-}bpy)PF_6)_3]^{2+/3+}$; (**B**) comparison of colors of cobalt- and iodine-based electrolytes; (**C**) time-course variation of photovoltaic parameters (averaged on five cells) for DSCs based on a $Co((MeIm\text{-}bpy)PF_6)_3]^{2+/3+}$-laden binary ionic liquid electrolyte. Adapted and reprinted with permission from [61].

3. Polymeric Matrices-Based Electrolytes Containing Cobalt Complexes

In view of the commercialization and large-scale deployment of DSCs, the widely-used organic solvents, such as ACN and MPN, have the concrete drawbacks of volatility and fluidity, which could

realistically result in evaporation and leakage during long-term usage. As a viable solution, DSCs based on a gel electrolyte can compete with their liquid counterparts in terms of PCE, and importantly, they have been reported to exhibit (in the presence of the standard iodide/triiodide redox couple) better long-term stability [63–67]. Gelled polymer electrolytes are highly interesting systems due to their facile preparation, as well as excellent liquid trapping capability [68–72]. Moreover, gelation offers the advantage of minimizing electrolyte leakage over time, while maintaining good contact between the dye molecules and the redox mediator. Last but not least, the DSSC community can take advantage of the recent strong advances carried out in the field of polymer science and technology [73–79] to achieve the best performance and stability in the resulting devices.

Spiccia and coworkers proposed cobalt-based gel electrolytes with 4 to 10 wt% of poly(vinylidene fluoride-*co*-hexafluoropropylene) (PVDF-HFP) incorporated in ACN [80]. Rheological characterization showed that 4 wt% of PVDF-HFP already assisted in the formation of a viscous gel structure. In order to ensure a good penetration of the electrolyte into the pores of the mesoporous photoanode, a backfilling technique was used to inject the warmed still-liquid PVDF-HFP electrolyte into the device. The gelation occurred *in situ* (inside the TiO_2 pores) in around 5 h. Devices sensitized with MK2 dye and assembled with 4% PVDF-HFP in ACN showed efficiencies of 8.7% under full sunlight intensity; J_{sc} and FF decreased when the polymer content was increased up to 10%. This suggested that an increase in the polymer content reduced the diffusion rate of the redox mediator, also slowing down the regeneration of dye molecules. Indeed, electrochemical measurements showed that the apparent diffusion coefficient (D_{app}) of $[Co(bpy)_3]^{3+}$ (1.39×10^{-6} $cm^2 \cdot s^{-1}$ for the liquid-state device, PCE = 10%) decreased by 30% when 4 wt% of PDVF-HFP was introduced and by 50% when 10 wt% of polymer was added.

As regards the long-term stability, cells were studied under continuous one sun illumination by white light LEDs (Figure 6). The device containing 4 wt% PDVF-HFP retained 90% of its initial PCE after 700 h, while the liquid-state cell maintained 90% of the initial efficiency for less than 200 h and then dropped to 25% of its original value after 500 h. This was caused by an enhanced decrease in J_{sc}, ascribed to the partial evaporation of the solvent.

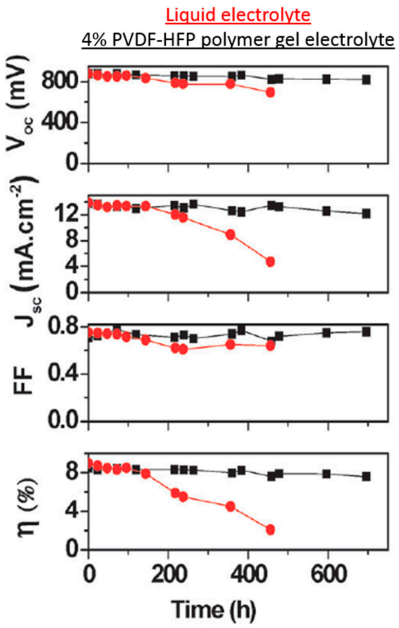

Figure 6. Stability test of liquid- and polymer gel electrolyte-based DSCs under one sun continuous illumination. Adapted and reprinted with permission from [80].

A similar poly(vinylidene fluoride) (PVDF)-based polymeric matrix was proposed by Kloo's group as a robust macromolecular cage for a cobalt-based redox couple [81]. Indeed, electrolytes

containing such a polymer are expected to have a very high stability due to the strong electron withdrawing –CF functional group, also accompanied by the higher degree of ion-pair dissociation promoted by this material, leading to a higher concentration of charge carriers. For this purpose, PVDF was dissolved (1.5 wt%) in a cobalt-based MPN electrolyte by stirring at 120 °C for 2.5 h and then injected through a pre-drilled hole in the counter-electrode glass substrates. Liquid electrolyte cells sensitized with D35 dye displayed an efficiency of 5.6% (J_{sc} = 10.2 mA cm^{-2}, V_{oc} = 0.94 V, FF = 0.57), while polymeric ones achieved a PCE of 6.4% (J_{sc} = 11.9 mA cm^{-2}, V_{oc} = 0.91 V, FF = 0.60) under one sun irradiation. The fabricated cells were kept under ambient conditions, in the dark and did not show loss in conversion efficiency, even after 1000 h.

Electrochemical investigations revealed that the polymer-based cell showed an enhanced electron lifetime, thus indicating lower recombination losses with respect to its liquid counterpart. Moreover, in charge extraction experiments, the solar cells containing PVDF displayed significantly higher amounts of collected charge and higher electron injection; the latter being due to the relatively high dielectric constant of PVDF, which can assist in greater ionization of cobalt salts, thus providing a high concentration of charge carriers. D_{app} values of the cobalt redox mediators were found from diffusion-limiting current experiments based on slow-scan cyclic voltammetry and were calculated for $[Co(bpy)_3]^{3+}$ to be 1.82 × 10^{-6} and 4.10 × 10^{-6} cm^2·s^{-1} in the liquid and polymeric electrolytes, respectively. It is highly interesting to note that the PVDF-based cell showed better ionic diffusion than the standard liquid cell. EIS showed that both cells displayed nearly the same resistance at the FTO surface (R_s) and at the counter electrode (R_{ce}); on the other hand, a marked difference was observed in R_{ct}, suggesting that recombination is more probable in PVDF-based devices.

Although PVDF and PVDF-HFP demonstrated good compatibility, efficiency and stability towards cobalt complex gelification, they present several disadvantages. First, these high molecular weight polymers require high temperature (100 to 150 °C) and time-consuming procedures to be dissolved in nitrile-based solvents, which is not favorable in terms of device cost and industrial scalability. Furthermore, these polymeric gels are usually prepared *ex situ*, and the proper impregnation of the active material particles into the mesopores of the photoanode is often hypothesized, but hardly ever demonstrated. For this purpose, a viable alternative would be the *in situ* photopolymerization of polymer electrolytes incorporating the Co(II)/Co(III)-based mediator. Indeed, photopolymerization is the preparation technique closest to the industrial requirements for DSC manufacturing, since it does not require solvents, catalysts and purification/separation steps [63,67,82–84].

As a first example of light-cured cobalt-based electrolyte, Bella *et al.* embedded the $[Co(bpy)_3]^{3+/2+}$ mediator in UV-crosslinkable methacrylic oligomers bearing ethoxy chains [63]. In detail, bisphenol A ethoxylate dimethacrylate (BEMA, M_n = 1700) and poly(ethylene glycol) methyl ether methacrylate (PEGMA, M_n = 700) were mixed with the cobalt complex and a free-radical photoinitiator (Irgacure 1173). The resulting mixture was introduced in a pre-sealed DSC via vacuum back-filling. The cell was UV-irradiated from the counter-electrode side for 1 min, allowing the methacrylic double bond conversion through photoinduced radical polymerization. Therefore, the dimethacrylate oligomer BEMA formed a crosslinked network, while PEGMA worked as a reactive diluent. The effective penetration of the newly-proposed polymer electrolyte in mesoporous photoanodes with different thicknesses (screen-printed on Pt-coated FTO substrates) was assessed by EIS, measuring R_{ce}. These values remained nearly constant with increasing film thickness up to 7 μm, thus indicating that the UV-cured electrolyte may efficiently permeate the film through its entire thickness.

Despite a lower J_{sc} value, the overall PCE of the quasi-solid (BEMA:PEGMA-based) cell was slightly higher if compared to the corresponding liquid counterpart under one sun irradiation (6.6 *vs.* 6.4%, respectively, sensitized with LEG4 dye, *i.e.*, 3-{6-{4-[bis(2′,4′-dibutyloxybiphenyl-4-yl)amino-]phenyl}-4,4-dihexyl-cyclopenta-[2,1-b:3,4-b′]dithiophene-2-yl}-2-cyanoacrylic acid). The quasi-solid device showed a higher V_{oc}, as expected by the suppression of dark current by polymer chains covering the TiO_2 nanoparticles surface. The stability of the cobalt-based DSCs was assessed by means of an 1800-h aging test. In the first 1500 h, cells were kept at a temperature of 60 °C in the dark,

and the resulting curves are shown in Figure 7A. The liquid cell was able to retain 42% of its initial PCE, while the cell assembled by *in situ* photopolymerization showed a very limited (5%) decay of the initial efficiency, thus demonstrating that the prepared polymeric network was able to effectively trap and retain the solvated Co(II)/Co(III) complex. In the second part of the aging experiment, cells were kept under continuous irradiation (one sun, without a UV filter) and thermostated at 40 °C. As clearly visible in the right portion of Figure 7B, the irradiation increased the speed of the degradative phenomena. Such an acceleration was attributed primarily to the UV component present in the radiation provided by the light source used in the experiment. Moreover, the chemical structure of cobalt-based redox mediators resembles that of photoinitiators for cationic photopolymerization, which are species able to absorb UV light and generate superacids harmful to the cell component. Overall, the degradation rate for the liquid device was ten-times higher than the polymeric one. This was attributed to the presence of a three-dimensional polymer network surrounding the redox mediator, since such a PEGylated architecture acted as a UV-absorber preventing the photodegradation of the cobalt-based redox mediator.

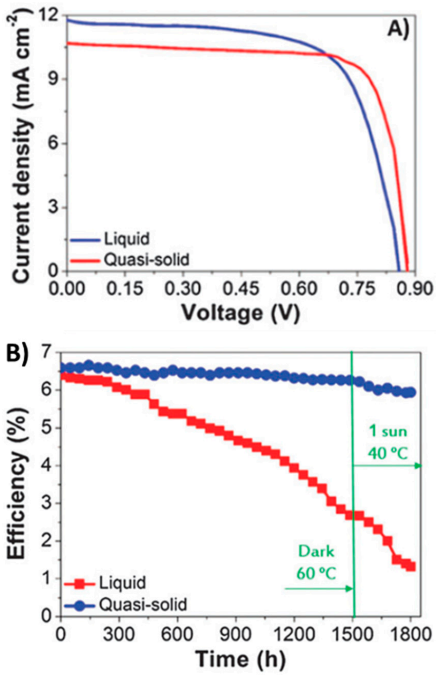

Figure 7. (**A**) J-V curves under one sun for DSCs assembled with Co(II)/Co(III) complex-based liquid or polymer electrolytes; (**B**) long-term stability of the same DSCs: 60 °C under dark conditions in the initial 1500 h and 40 °C at one sun without a UV filter from 1500 to 1800 h. Adapted and reprinted with permission from [63].

4. Inorganic Gel-Based Electrolytes Containing Cobalt Complexes

As an alternative to polymers, inorganic nanoparticles have been shown to be valid gelification agents of liquid electrolytes when used in the presence of the iodine-based redox pair [85–87]. Furthermore, it has been shown that in particular concentration ranges, the nanoparticles organize themselves so as to form preferential channels for ions mobility, the latter being a fundamental factor to limit the typical mass diffusion phenomena observed in the presence of quasi-solid electrolytes.

In order to improve the long-term stability and lifetime of DSC devices, Stergiopoulos and coworkers proposed an innovative solidified redox electrolyte by incorporating amorphous silica nanoparticles in a liquid system containing the Co^{2+}/Co^{3+} shuttle as redox mediator [88]. In detail, a liquid cobalt-based electrolyte containing [Co-$(bpy)_3(PF_6)_2$] 0.22 M, [$Co(bpy)_3(PF_6)_3$] 33 mM, $LiClO_4$ 0.10 M and TBP 0.20 M dissolved in MPN was solidified by adding an amount of silica nanoparticles

(5 wt%) under continuous stirring, in order to obtain quasi-solid DSCs. Quasi-solid devices, sensitized with organic D35 dye, were fabricated by incorporating this electrolyte and attained an efficiency of 2.6% under one sun irradiation, corresponding to the 73% of the PCE measured for the reference liquid electrolyte (Table 1). The authors also noted that cell efficiency depended on the illumination intensity and significantly increased up to more than 4% under 0.23 sun. This value represented a very important result if one considers that it was the first ever literature report in which a solidified electrolyte based on the Co(II)/(III) couple was presented. In detail, the relatively lower efficiency of the quasi-solid DSC was ascribed to reduced J_{sc} and slightly lower FF with respect to the liquid device. Linear sweep voltammetry and EIS experiments on thin symmetrical cells incorporating liquid and solidified electrolytes demonstrated that the 25% decrease of the photocurrent was assigned to the reduced values of ionic conductivity and diffusion of the Co^{3+} cations. Overall, it should also be stated that both the electrolytes showed decreased ions diffusion and mass transport above 0.5 sun, with large deviations from linearity, suggesting that these redox active species require a more porous TiO_2 structure to better diffuse in the photoelectrode. On the other hand, the lower FF of the quasi-solid cell was attributed to increased series resistance due to the increased diffusion impedance of the electrolyte. The only parameter where the quasi-solid device outperformed the liquid counterpart was the V_{oc}; indeed, it reached the impressive value of 0.86 V, probably due to a significant shift of the dark current towards negative potentials (−57 mV) for the solidified electrolyte. The authors attributed this evidence to a negative shift of the TiO_2 conduction band edge, caused by its interaction with small negatively-charged silica nanoparticles. Moreover, this small negative shift could also affect electron injection by the excited dye on the semiconductor by reducing the underlying driving force [89] and leading to a further decrease in J_{sc}.

Table 1. Electrical parameters derived from J-V curves on DSCs based on liquid and solidified electrolytes, under different levels of light illumination. Adapted and reprinted with permission from [88].

Electrolyte	Illumination Intensity (sun)	J_{sc} (mA cm^{-2})	V_{oc} (mV)	FF	PCE (%)
Liquid	1	6.42	836	0.66	3.52
	0.5	4.44	811	0.64	4.60
	0.23	2.17	787	0.65	4.79
	0.1	0.99	755	0.62	4.65
Solidified	1	4.76	855	0.63	2.58
	0.5	3.63	834	0.59	3.58
	0.23	1.84	817	0.62	4.03
	0.1	0.84	787	0.62	4.07

5. Aqueous Electrolytes: An Emerging Approach to Stabilize Cobalt Complexes

The use of organic solvents for the preparation of DSC electrolytes is problematic, since they are generally highly toxic and flammable. On the other hand, water as the most abundant and benign solvent on Earth and is ideal for the preparation of DSC electrolytes; several research groups have recently turned their interest toward this direction [55,70,90–94]. Another drawback, typical of quasi-solid DSCs, concerns the effect of the poor penetration of gel electrolytes into the mesoporous photoanodes [95]. For this purpose, a viable solution is the replacement of the standard nanocrystalline photoanode with submicrometer-sized mesoporous TiO_2 beads [96]. Indeed, even if beads have larger pores and a smaller surface area, the resulting electrode leads to improved diffusion of the cobalt complexes inside the oxide layer.

Aqueous gel electrolytes and modified photoanodes for stable cobalt-based DSCs were investigated simultaneously by Spiccia's group [97]. Each electrode was composed of a 1 mm-thick transparent titania layer (30 nm TiO_2 particles) and a 4 mm-thick scattering layer comprised of either: (i) 80 wt% of 400 nm TiO_2 and 20 wt% of 18 nm TiO_2 nanoparticles (named the CCIC electrode);

or (ii) SP33-800 mesoporous beads (*i.e.*, titania beads of 800 ± 40 nm with 33-nm mesopores); or (iii) SP46-800 mesoporous beads (*i.e.*, titania beads of 800 ± 40 nm with 46-nm mesopores). In their work, gelatin (*i.e.*, a polypeptide made by hydrolytic degradation of collagen) was employed as the gelator in the preparation of aqueous DSCs based on the $[Co(bpy)_3]^{2+/3+}$ mediator. Gelatin was highly water-soluble (15 wt%), and gelation was sufficiently slow to allow good penetration of the liquid precursor electrolyte into the TiO_2 film before the *in situ* solidification took place inside the mesopores.

For the devices made with the CCIC scattering layer, a J_{sc} of 1.09 mA cm^{-2} and a PCE of 4.9% were obtained under 0.1 sun illumination; however, the increase in J_{sc} with the light intensity was not linear (Figure 8B), and only 3.0% PCE was measured at one sun intensity. On the other hand, cells with SP33-800 and SP46-800 scattering layers exceeded the performance of the CCIC-based devices at one sun irradiation, reaching a J_{sc} of 7.9 mA cm^{-2} and a PCE of 4.1%. The effect of pore size on mass transport was further investigated by photocurrent transient measurements employing a modulation of the incident light. At elevated light intensities, all of the three devices showed a diffusion-limitation behavior (Figure 8A): indeed, the photocurrent spiked and then took some time to stabilize, indicating that charge-carrier transport was retarded and photocurrent generation was limited. Overall, the plot suggested that TiO_2 beads with the largest pores were more suitable for use in conjunction with aqueous gel electrolytes.

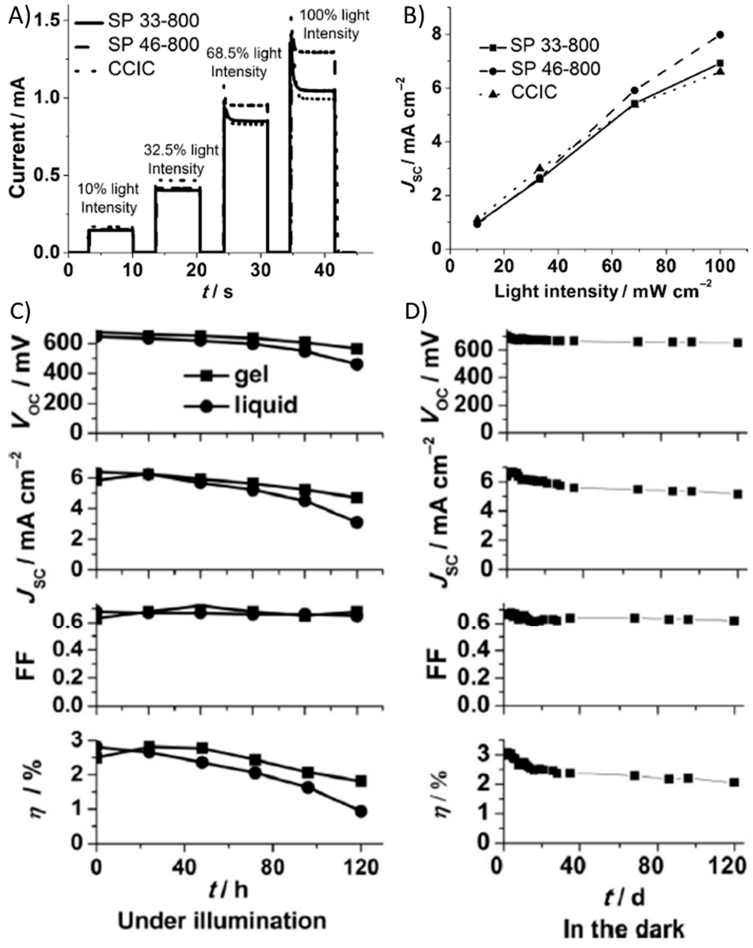

Figure 8. (**A**) Photocurrent transient measurements on DSCs assembled with one of three scattering layers on the different working electrodes. The illumination on/off ratio was fixed at two, which means that the cells were illuminated for 7 s following 3.5 s without illumination. (**B**) Dependence of J_{sc} on light intensity for the three DSCs. (**C**) Performance parameters comparing the stability of the aqueous gel and liquid DSCs under one sun illumination and (**D**) when stored in the dark. Adapted and reprinted with permission from [97].

In order to investigate DSCs stability, quasi-solid and liquid devices were exposed under white LED light illumination (one sun; Figure 8C). For gel-electrolyte-based devices, the V_{oc} slightly decreased upon illumination, whereas in the first 20 h the J_{sc} continuously decreased, and dye desorption from the TiO_2 was identified as the main reason for this behavior. Overall, the quasi-solid device maintained over 80% of its original efficiency after illumination for 90 h, whereas the value for liquid counterparts was 57%, suggesting that the stability for the gelified electrolytes was promising. In a second experiment, cells were stored under dark conditions and degradation proceeded more slowly (Figure 8D): 80% of the initial PCE was retained after 35 days for the quasi-solid device, which maintained 75% of the original performance up to 120 days.

The aqueous $[Co(bpy)_3]^{2+/3+}$ redox couple was also tested in the presence of a donor–π–acceptor dye (MK2) by Xiang *et al.* [98]. Device efficiencies of 3.7% were achieved and were then significantly improved by the introduction of small amounts of poly(ethylene glycol) (PEG) to the electrolyte solution. Addition of 1 wt% PEG 300 resulted in device efficiencies of 4.2%. Moreover, by replacing Pt counter electrodes with indium tin oxide (ITO)/Pt counter electrodes, a PCE equal to 5.1% was measured. These devices exhibited excellent stability on storage for 90 days, while under one sun illumination, they lost 30% of the initial efficiency in 60 h. This means that the stability of aqueous cobalt-based DSSCs still needs to be highly improved by the scientific community.

We think that many other advances can be made in the field of aqueous DSSCs containing redox mediators based on cobalt complexes, also exploiting recently-proposed materials in the solar cell field, such as metal-organic frameworks [99,100], zinc oxide nanoparticles [101–107], electrochromic [108] and luminescent agents [109,110].

6. Conclusions

In this review, we have proposed the recent trends aimed at the stabilization of DSCs containing cobalt-based electrolytes. This redox mediator has enabled DSCs to achieve efficiencies higher than 14% (competitive with those of perovskite solar cells [111,112]), but often not stable over time.

A first strategy for the improvement of the stability is the design of thermodynamically-stable molecular structures, not photosensitive and not suffering from ligands exchange with other components present in the electrolyte. A further stabilization technique of cobalt-based DSCs is focused on the increase of the concentration of the redox mediator, together with the adoption of small amounts of bases (such as TBP), also useful to increase the photovoltage.

A second approach is aimed at replacing the organic solvent-based liquid electrolyte with either a polymeric matrix, an ionic liquid or gellified inorganic nanoparticles. In these systems, the penetration of the quasi-solid electrolyte in the electrode must be maximized, and filling technologies or *in situ* polymerization methods leading to an excellent electrode/electrolyte interface have been proposed.

Finally, cobalt-based redox couples are finding very good synergy with water-based electrolytes, which represent an emerging trend in the DSC field. Water-based electrolytes would represent the perfect solution for implementing these cells in close contact with humans, such as in indoor devices, embedded in textiles or as smart windows in houses.

Globally, the scientific community has recently demonstrated that the performance of cobalt-based solar cells might be stabilized, but this has often led to a strong reduction of the efficiencies measured in the liquid state. It is therefore fundamental to proceed further with intensive research efforts in order to achieve both the goals of high efficiency and long-term stability.

Acknowledgments: Quelli-Di-Luglio (QdL) members are warmly thanked for the continuous and useful scientific discussions.

Author Contributions: F.B. conceived the work. F.B. and S.G. did bibliographic research and organized the drafting of the manuscript. C.G. and G.V. supervised the work and balanced the contents of this review. All of the authors contributed to the improvement of the manuscript during the peer-review process.

Conflicts of Interest: The authors declare no conflict of interest.

Abbreviations

The following abbreviations are used in this manuscript:

ACN	Acetonitrile
bpy	Bipyridine
bpyPY4	6,6′-bis(1,1-di(pyridin-2-yl)ethyl)-2,2′-bipyridine
BEMA	Bisphenol A ethoxylate dimethacrylate
BIm^+	1-butyl-3-methylimidazolium ion
$CF_3SO_3^-$	Trifluoromethanesulfonate ion
cn-bpy	2,2′-bipyridine-4,4′-dicarbonitrile
D21L6	(E)-3-(5-(5-(4-(bis(4-(hexyloxy)phenyl)thiophene-2-yl)thiophene-2-yl)-2-cyanoacrylic acid
D25L6	(E)-3-(5-(5-(4-(bis(4-(dodecyloxy)phenyl)thiophene-2-yl)thiophene-2-yl)- 2-cyanoacrylic acid
D35	(E)-3-(5-(4-(bis(2',4'-dibutoxy-[1,1'-biphenyl]-4-yl)amino)phenyl)thiophen-2-yl)-2-cyanoacrylic acid
D_{app}	Apparent diffusion coefficient
dma-bpy	2,2′-bipyridine-4,4′-bis(N,N-dimethylcarboxamide)
DSC	Dye-sensitized solar cell
EIS	Electrochemical impedance spectroscopy
EIm^+	1-ethyl-3-methylimidazolium ion
EMINCS	1-ethyl-3-methylimidazolium thiocyanate
FF	Fill-factor
GuNCS	Guanidinium thiocyanate
ITO	Indium tin oxide
J_{sc}	Short-circuit photocurrent density
LEG4	3-{6-{4-[bis(2′,4′-dibutyloxybiphenyl-4-yl)amino-]phenyl}-4,4-dihexyl-cyclopenta-[2,1-b:3,4-b′]dithiophene-2-yl}-2-cyanoacrylic acid
LiTFSI	Bis(trifluoromethane)sulfonimide lithium salt
me-bpy	2,2′-bipyridine-4,4′-bis(methyl ester)
$(MeIm\text{-}bpy)PF_6)_3$	3,3′-(2,2′-bipyridine-4,4′-diylbis(methylene))bis(1-methyl-1H-imidazol-3-ium) hexafluorohosphate)
MK2	2-cyano-3-[5′′′-(9-ethyl-9*H*-carbazol-3-yl)-3′,3′′,3′′′,4-tetra-*n*-hexyl-[2,2′,5′,2′′,5′′,2′′′]-quater thiophen-5-yl] acrylic acid
MPN	3-methoxypropionitrile
NCPV	National Center for Photovoltaics
NMBI	1-methylbenzimidazole
$NOBF_4$	Nitrosonium tetrafluoroborate
NREL	National Renewable Energy Laboratory
N719	Di-tetrabutylammonium *cis*-bis(isothiocyanato)bis(2,2′-bipyridyl-4,4′-dicarboxylato) ruthenium(II)
PCE	Power conversion efficiency
PEG	Poly(ethylene glycol)
PEGMA	Poly(ethylene glycol) methyl ether methacrylate
PMII	1-propyl-3-methylimidazolium iodine
PVDF	Poly(vinylidene fluoride)
PVDF-HFP	Poly(vinylidene fluoride-*co*-hexafluoropropylene)
R_{ce}	Resistance at the counter electrode
R_{ct}	Charge transfer resistance at the photoanode/electrolyte interface
R_d	Diffusion resistance of the electrolyte
R_s	Resistance at the FTO surface
SSCE	Saturated salt calomel electrode
TBA^+	Tetrabutyl cation
TBP	4-*tert*-butylpyridine
TEA^+	Tetraethylammonium ion
TFMP	*p*-trifluoromethylpyridine
V_{oc}	Open circuit potential
Z907	*cis*-bis(isothiocyanato)(2,2′-bipyridyl-4,4′-dicarboxylato)(4,4′-di-nonyl-2′-bipyridyl) ruthenium(II)

References

1. Kakiage, K.; Aoyama, Y.; Yano, T.; Oya, K.; Fujisawa, J.I.; Hanaya, M. Highly-Efficient Dye-Sensitized Solar Cells with Collaborative Sensitization by Silyl-Anchor and Carboxy-Anchor Dyes. *Chem. Commun.* **2015**, *51*, 15894–15897.
2. Karamshuk, S.; Caramori, S.; Manfredi, N.; Salamone, M.; Ruffo, R.; Carli, S.; Bignozzi, C.A.; Abbotto, A. Molecular Level Factors Affecting the Efficiency of Organic Chromophores for p-Type Dye Sensitized Solar Cells. *Energies* **2016**, *9*. [CrossRef]
3. De Rossi, F.; Pontecorvo, T.; Brown, T.M. Characterization of Photovoltaic Devices for Indoor Light Harvesting and Customization of Flexible Dye Solar Cells to Deliver Superior Efficiency under Artificial Lighting. *Appl. Energy* **2015**, *156*, 413–422.
4. Mastroianni, S.; Lanuti, A.; Penna, S.; Reale, A.; Brown, T.M.; Di Carlo, A.; Decker, F. Physical and Electrochemical Analysis of an Indoor-Outdoor Ageing Test of Large-Area Dye Solar Cell Devices. *ChemPhysChem* **2012**, *13*, 2925–2936.
5. Heiniger, L.P.; O'Brien, P.G.; Soheilnia, N.; Yang, Y.; Kherani, N.P.; Grätzel, M.; Ozin, G.A.; Tétreault, N. See-Through Dye-Sensitized Solar Cells: Photonic Reflectors for Tandem and Building Integrated Photovoltaics. *Adv. Mater.* **2013**, *25*, 5734–5741.
6. Yu, M.; McCulloch, W.D.; Huang, Z.; Trang, B.B.; Lu, J.; Amine, K.; Wu, Y. Solar-Powered Electrochemical Energy Storage: An Alternative to Solar Fuels. *J. Mater. Chem. A* **2016**, *4*, 2766–2782.
7. Yu, Z.; Vlachopoulos, N.; Gorlov, M.; Kloo, L. Liquid Electrolytes for Dye-Sensitized Solar Cells. *Dalton Trans.* **2011**, *40*, 10289–10303. [PubMed]
8. Wang, M.; Grätzel, C.; Zakeeruddin, S.M.; Grätzel, M. Recent Developments in Redox Electrolytes for Dye-Sensitized Solar Cells. *Energy Environ. Sci.* **2012**, *5*, 9394–9405.
9. Yun, S.; Lund, P.D.; Hinsch, A. Stability Assessment of Alternative Platinum Free Counter Electrodes for Dye-Sensitized Solar Cells. *Energy Environ. Sci.* **2015**, *8*, 3495–3514.
10. Yue, G.; Yang, G.; Li, F.; Wu, J. PEDOT: PSS Assisted Preparation of a Graphene/Nickel Cobalt Oxide Hybrid Counter Electrode to Serve in Efficient Dye-Sensitized Solar Cells. *RSC Adv.* **2015**, *5*, 100159–100168.
11. Wan, L.; Luo, T.; Wang, S.; Wang, X.; Guo, Z.; Xiong, H.; Dong, B.; Zhao, L.; Xu, Z.; Zhang, X.; *et al.* Pt/Graphene Nanocomposites with Low Pt-Loadings: Synthesis through One- and Two-Step Chemical Reduction Methods and Their Use as Promising Counter Electrodes for DSSCs. *Compos. Sci. Technol.* **2015**, *113*, 46–53. [CrossRef]
12. Song, D.; Cho, W.; Lee, J.H.; Kang, Y.S. Toward Higher Energy Conversion Efficiency for Solid Polymer Electrolyte Dye-Sensitized Solar Cells: Ionic Conductivity and TiO_2 Pore-Filling. *J. Phys. Chem. Lett.* **2014**, *5*, 1249–1258. [CrossRef] [PubMed]
13. Ye, M.; Wen, X.; Wang, M.; Iocozzia, J.; Zhang, N.; Lin, C.; Lin, Z. Recent Advances in Dye-Sensitized Solar Cells: From Photoanodes, Sensitizers and Electrolytes to Counter Electrodes. *Mater. Today* **2015**, *18*, 155–162. [CrossRef]
14. Wu, J.; Lan, Z.; Lin, J.; Huang, M.; Huang, Y.; Fan, L.; Luo, G. Electrolytes in Dye-Sensitized Solar Cells. *Chem. Rev.* **2015**, *115*, 2136–2173. [CrossRef] [PubMed]
15. O'Regan, B.; Grätzel, M. A Low-Cost, High-Efficiency Solar Cell based on Dye-Sensitized Colloidal TiO_2 Films. *Nature* **1991**, *353*, 737–740. [CrossRef]
16. Grätzel, M. Dye-Sensitized Solar Cells. *J. Photochem. Photobiol. C* **2003**, *4*, 145–153. [CrossRef]
17. Cong, J.; Yang, X.; Kloo, L.; Sun, L. Iodine/Iodide-Free Redox Shuttles for Liquid Electrolyte-Based Dye-Sensitized Solar Cells. *Energy Environ. Sci.* **2012**, *5*, 9180–9194. [CrossRef]
18. Maza, W.A.; Haring, A.J.; Ahrenholtz, S.R.; Epley, C.C.; Lin, S.Y.; Morris, A.J. Ruthenium(II)-Polypyridyl Zirconium(IV) Metal-Organic Frameworks as a New Class of Sensitized Solar Cells. *Chem. Sci.* **2015**, *7*, 719–727. [CrossRef]
19. Gao, H.H.; Qian, X.; Chang, W.Y.; Wang, S.S.; Zhu, Y.Z.; Zheng, J.Y. Oligothiophene-Linked D-p-A Type Phenothiazine Dyes for Dye-Sensitized Solar Cells. *J. Power Sources* **2016**, *307*, 866–874. [CrossRef]
20. Su, H.C.; Wu, Y.Y.; Hou, J.L.; Zhang, G.L.; Zhu, Q.Y.; Dai, J. Dye Molecule Bonded Titanium Alkoxide: A Possible New Type of Dye for Sensitized Solar Cells. *Chem. Commun.* **2016**, *52*, 4072–4075. [CrossRef] [PubMed]

21. Giribabu, L.; Bolligarla, R.; Panigrahi, M. Recent Advances of Cobalt(II/III) Redox Couples for Dye-Sensitized Solar Cell Applications. *Chem. Rec.* **2015**, *15*, 760–788. [CrossRef] [PubMed]
22. Klahr, B.M.; Hamann, T.W. Performance Enhancement and Limitations of Cobalt Bipyridyl Redox Shuttles in Dye-Sensitized Solar Cells. *J. Phys. Chem. C* **2009**, *113*, 14040–14045. [CrossRef]
23. Tsao, H.N.; Yi, C.; Moehl, T.; Yum, J.H.; Zakeeruddin, S.M.; Nazeeruddin, M.K.; Grätzel, M. Cyclopentadithiophene Bridged Donor-Acceptor Dyes Achieve High Power Conversion Efficiencies in Dye-Sensitized Solar Cells Based on the Tris-Cobalt Bipyridine Redox Couple. *ChemSusChem* **2011**, *4*, 591–594. [CrossRef] [PubMed]
24. Sapp, S.A.; Elliott, C.M.; Contado, C.; Caramori, S.; Bignozzi, C.A. Substituted Polypyridine Complexes of Cobalt(II/III) as Efficient Electron-Transfer Mediators in Dye-Sensitized Solar Cells. *J. Am. Chem. Soc.* **2002**, *124*, 11215–11222. [CrossRef] [PubMed]
25. Feldt, S.M.; Gibson, E.A.; Gabrielsson, E.; Sun, L.; Boschloo, G.; Hagfeldt, A. Design of Organic Dyes and Cobalt Polypyridine Redox Mediators for High-Efficiency Dye-Sensitized Solar Cells. *J. Am. Chem. Soc.* **2010**, *132*, 16714–16724. [CrossRef] [PubMed]
26. Harikisun, R.; Desilvestro, H. Long-Term Stability of Dye Solar Cells. *Sol. Energy* **2011**, *85*, 1179–1188. [CrossRef]
27. Asghar, M.I.; Miettunen, K.; Halme, J.; Vahermaa, P.; Toivola, M.; Aitola, K.; Lund, P. Review of Stability for Advanced Dye Solar Cells. *Energy Environ. Sci.* **2010**, *3*, 418–426. [CrossRef]
28. Sommeling, P.M.; Späth, M.; Smit, H.J.P.; Bakker, N.J.; Kroon, J.M. Long-Term Stability Testing of Dye-Sensitized Solar Cells. *J. Photochem. Photobiol. A* **2004**, *164*, 137–144. [CrossRef]
29. Hinsch, A.; Kroon, J.M.; Kern, R.; Uhlendorf, I.; Holzbock, J.; Meyer, A.; Ferber, J. Long-Term Stability of Dye-Sensitised Solar Cells. *Prog. Photovoltaics Res. Appl.* **2001**, *9*, 425–438. [CrossRef]
30. National Center for Photovoltaics (NCPV) at the National Renewable Energy Laboratory (NREL). Available online: http://www.nrel.gov/ncpv (accessed on 8 April 2016).
31. Kirner, J.T.; Elliott, C.M. Are High-Potential Cobalt Tris(bipyridyl) Complexes Sufficiently Stable to Be Efficient Mediators in Dye-Sensitized Solar Cells? Synthesis, Characterization, and Stability Tests. *J. Phys. Chem. C* **2015**, *119*, 17502–17514. [CrossRef]
32. Izatt, R.M.; Pawlak, K.; Bradshaw, J.S.; Bruening, R.L. Thermodynamic and Kinetic Data for Macrocycle Interaction with Cations and Anions. *Chem. Rev.* **1991**, *91*, 1721–2085. [CrossRef]
33. Endicott, J.F.; Brubaker, G.R.; Ramasami, T.; Kumar, K.; Dwarakanath, K.; Cassel, J.; Johnson, D. Electron-Transfer Reactivity in Some Simple Cobalt(III)-Cobalt(II) Couples. Franck-Condon *vs*. Electronic Contributions. *Inorg. Chem.* **1983**, *22*, 3754–3762. [CrossRef]
34. Kashif, M.K.; Nippe, M.; Duffy, N.W.; Forsyth, C.M.; Chang, C.J.; Long, J.R.; Spiccia, L.; Bach, U. Stable Dye-Sensitized Solar Cell Electrolytes Based on Cobalt(II)/(III) Complexes of a Hexadentate Pyridyl Ligand. *Angew. Chem. Int. Ed.* **2013**, *52*, 5527–5531. [CrossRef] [PubMed]
35. García-Monforte, M.A.; Martínez-Salvador, S.; Menjõn, B. The Trifluoromethyl Group in Transition Metal Chemistry. *Eur. J. Inorg. Chem.* **2012**, *31*, 4945–4966. [CrossRef]
36. Mosconi, E.; Yum, J.H.; Kessler, F.; Gómez García, C.J.; Zuccaccia, C.; Cinti, A.; Nazeeruddin, M.K.; Grätzel, M.; De Angelis, F. Cobalt Electrolyte/Dye Interactions in Dye-Sensitized Solar Cells: A Combined Computational and Experimental Study. *J. Am. Chem. Soc.* **2012**, *134*, 19438–19453. [CrossRef] [PubMed]
37. Pugliese, D.; Bella, F.; Cauda, V.; Lamberti, A.; Sacco, A.; Tresso, E.; Bianco, S. A Chemometric Approach for the Sensitization Procedure of ZnO Flowerlike Microstructures for Dye-Sensitized Solar Cells. *ACS Appl. Mater. Interfaces* **2013**, *5*, 11288–11295. [CrossRef] [PubMed]
38. Bella, F.; Imperiyka, M.; Ahmad, A. Photochemically Produced Quasi-Linear Copolymers for Stable and Efficient Electrolytes in Dye-Sensitized Solar Cells. *J. Photochem. Photobiol. A* **2014**, *289*, 73–80. [CrossRef]
39. Bella, F.; Sacco, A.; Pugliese, D.; Laurenti, M.; Bianco, S. Additives and Salts for Dye-Sensitized Solar Cells Electrolytes: What is the Best Choice? *J. Power Sources* **2014**, *264*, 333–343. [CrossRef]
40. Gianotti, V.; Favaro, G.; Bonandini, L.; Palin, L.; Croce, G.; Boccaleri, E.; Artuso, E.; Van Beek, W.; Barolo, C.; Milanesio, M. Rationalization of Dye Uptake on Titania Slides for Dye-Sensitized Solar Cells by a Combined Chemometric and Structural Approach. *ChemSusChem* **2014**, *7*, 3039–3052. [CrossRef] [PubMed]
41. Enciso, P.; Cerdá, M.F. Solar Cells based on the Use of Photosensitizers Obtained from Antarctic Red Algae. *Cold Reg. Sci. Technol.* **2016**, *126*, 51–54. [CrossRef]

42. Qian, X.; Shao, L.; Li, H.; Yan, R.; Wang, X.; Hou, L. Indolo[3,2-b]Carbazole-based Multi-Donor-p-Acceptor Type Organic Dyes for Highly Efficient Dye-Sensitized Solar Cells. *J. Power Sources* **2016**, *319*, 39–47. [CrossRef]
43. O'Donnell, R.M.; Sampaio, R.N.; Li, G.; Johansson, P.G.; Ward, C.L.; Meyer, G.J. Photoacidic and Photobasic Behavior of Transition Metal Compounds with Carboxylic Acid Group(s). *J. Am. Chem. Soc.* **2016**, *138*, 3891–3903. [CrossRef] [PubMed]
44. Nakade, S.; Makimoto, Y.; Kubo, W.; Kitamura, T.; Wada, Y.; Yanagida, S. Roles of Electrolytes on Charge Recombination in Dye-Sensitized TiO_2 Solar Cells (2): The Case of Solar Cells Using Cobalt Complex Redox Couples. *J. Phys. Chem. B* **2005**, *109*, 3488–3493. [CrossRef] [PubMed]
45. Koh, T.M.; Nonomura, K.; Mathews, N.; Hagfeldt, A.; Grätzel, M.; Mhaisalkar, S.G.; Grimsdale, A.C. Influence of 4-tert-Butylpyridine in DSCs with $Co^{II/III}$ Redox Mediator. *J. Phys. Chem. C* **2013**, *117*, 15515–15522. [CrossRef]
46. Nakade, S.; Kanzaki, T.; Kambe, S.; Wada, Y.; Yanagida, S. Investigation of Cation-Induced Degradation of Dye-Sensitized Solar Cells for a New Strategy to Long-Term Stability. *Langmuir* **2005**, *21*, 11414–11417. [CrossRef] [PubMed]
47. Kontos, A.G.; Stergiopoulos, T.; Likodimos, V.; Milliken, D.; Desilvesto, H.; Tulloch, G.; Falaras, P. Long-Term Thermal Stability of Liquid Dye Solar Cells. *J. Phys. Chem. C* **2013**, *117*, 8636–8646. [CrossRef]
48. Likodimos, V.; Stergiopoulos, T.; Falaras, P.; Harikisun, R.; Desilvestro, J.; Tulloch, G. Prolonged Light and Thermal Stress Effects on Industrial Dye-Sensitized Solar Cells: A Micro-Raman Investigation on the Long-Term Stability of Aged Cells. *J. Phys. Chem. C* **2009**, *113*, 9412–9422.
49. Zhang, C.; Huang, Y.; Chen, S.; Tian, H.; Mo, L.; Hu, L.; Huo, Z.; Kong, F.; Ma, Y.; Dai, S. Photoelectrochemical Analysis of the Dyed TiO_2/Electrolyte Interface in Long-Term Stability of Dye-Sensitized Solar Cells. *J. Phys. Chem. C* **2012**, *116*, 19807–19813. [CrossRef]
50. Bandara, T.M.W.J.; Jayasundara, W.J.M.J.S.R.; Dissanayake, M.A.K.L.; Fernando, H.D.N.S.; Furlani, M.; Albinsson, I.; Mellander, B.E. Quasi Solid State Polymer Electrolyte with Binary Iodide Salts for Photo-Electrochemical Solar Cells. *Int. J. Hydrogen Energy* **2014**, *39*, 2997–3004.
51. Bandara, T.M.W.J.; Aziz, M.F.; Fernando, H.D.N.S.; Careem, M.A.; Arof, A.K.; Mellander, B.E. Efficiency Enhancement in Dye-Sensitized Solar Cells with a Novel PAN-based Gel Polymer Electrolyte with Ternary Iodides. *J. Solid State Electrochem.* **2015**, *19*, 2353–2359.
52. Gao, J.; Bhagavathi Achari, M.; Kloo, L. Long-Term Stability for Cobalt-Based Dye-Sensitized Solar Cells Obtained by Electrolyte Optimization. *Chem. Commun.* **2014**, *50*, 6249–6251.
53. Jiang, R.; Anderson, A.; Barnes, P.R.F.; Xiaoe, L.; Law, C.; O'Regan, B.C. 2000 Hours Photostability Testing of Dye Sensitised Solar Cells Using a Cobalt Bipyridine Electrolyte. *J. Mater. Chem. A* **2014**, *2*, 4751–4757.
54. Gao, J.; Yang, W.; Pazoki, M.; Boschloo, G.; Kloo, L. Cation-Dependent Photostability of Co(II/III)-Mediated Dye-Sensitized Solar Cells. *J. Phys. Chem. C* **2015**, *119*, 24704–24713.
55. Bella, F.; Gerbaldi, C.; Barolo, C.; Grätzel, M. Aqueous Dye-Sensitized Solar Cells. *Chem. Soc. Rev.* **2015**, *44*, 3431–3473.
56. Bai, Y.; Cao, Y.; Zhang, J.; Wang, M.; Li, R.; Wang, P.; Zakeeruddin, S.M.; Grätzel, M. High-Performance Dye-Sensitized Solar Cells Based on Solvent-Free Electrolytes Produced from Eutectic Melts. *Nat. Mater.* **2008**, *7*, 626–630.
57. Wang, P.; Wenger, B.; Humphry-Baker, R.; Moser, J.E.; Teuscher, J.; Kantlehner, W.; Mezger, J.; Stoyanov, E.V.; Zakeeruddin, S.M.; Grätzel, M. Charge Separation and Efficient Light Energy Conversion in Sensitized Mesoscopic Solar Cells Based on Binary Ionic Liquids. *J. Am. Chem. Soc.* **2005**, *127*, 6850–6856.
58. Wang, P.; Zakeeruddin, S.M.; Humphry-Baker, R.; Grätzel, M. A Binary Ionic Liquid Electrolyte to Achieve $\geqslant$7% Power Conversion Efficiencies in Dye-Sensitized Solar Cells. *Chem. Mater.* **2004**, *16*, 2694–2696.
59. Chen, X.; Zhao, J.; Zhang, J.; Qiu, L.; Xu, D.; Zhang, H.; Han, X.; Sun, B.; Fu, G.; Zhang, Y.; *et al.* Bis-Imidazolium Based Poly(Ionic Liquid) Electrolytes for Quasi-Solid-State Dye-Sensitized Solar Cells. *J. Mater. Chem.* **2012**, *22*, 18018–18024. [CrossRef]
60. Zhao, J.; Shen, X.; Yan, F.; Qiu, L.; Lee, S.; Sun, B. Solvent-Free Ionic Liquid/Poly(Ionic Liquid) Electrolytes for Quasi-Solid-State Dye-Sensitized Solar Cells. *J. Mater. Chem.* **2011**, *21*, 7326–7330. [CrossRef]
61. Xu, D.; Zhang, H.; Chen, X.; Yan, F. Imidazolium Functionalized Cobalt Tris(Bipyridyl) Complex Redox Shuttles for High Efficiency Ionic Liquid Electrolyte Dye-Sensitized Solar Cells. *J. Mater. Chem. A* **2013**, *1*, 11933–11941. [CrossRef]

62. Gibson, E.A.; Smeigh, A.L.; Le Pleux, L.; Hammarström, L.; Odobel, F.; Boschloo, G.; Hagfeldt, A. Cobalt Polypyridyl-Based Electrolytes for p-Type Dye-Sensitized Solar Cells. *J. Phys. Chem. C* **2011**, *115*, 9772–9779. [CrossRef]
63. Bella, F.; Vlachopoulos, N.; Nonomura, K.; Zakeeruddin, S.M.; Grätzel, M.; Gerbaldi, C.; Hagfeldt, A. Direct Light-Induced Polymerization of Cobalt-Based Redox Shuttles: An Ultrafast Way Towards Stable Dye-Sensitized Solar Cells. *Chem. Commun.* **2015**, *51*, 16308–16311. [CrossRef] [PubMed]
64. Bella, F. Polymer Electrolytes and Perovskites: Lights and Shadows in Photovoltaic Devices. *Electrochim. Acta* **2015**, *175*, 151–161. [CrossRef]
65. Gerosa, M.; Sacco, A.; Scalia, A.; Bella, F.; Chiodoni, A.; Quaglio, M.; Tresso, E.; Bianco, S. Toward Totally Flexible Dye-Sensitized Solar Cells Based on Titanium Grids and Polymeric Electrolyte. *IEEE J. Photovoltaics* **2016**, *6*, 498–505. [CrossRef]
66. Bella, F.; Chiappone, A.; Nair, J.R.; Meligrana, G.; Gerbaldi, C. Effect of Different Green Cellulosic Matrices on the Performance of Polymeric Dye-Sensitized Solar Cells. *Chem. Eng. Trans.* **2014**, *41*, 211–216.
67. Bella, F.; Sacco, A.; Massaglia, G.; Chiodoni, A.; Pirri, C.F.; Quaglio, M. Dispelling Clichés at the Nanoscale: the True Effect of Polymer Electrolytes on the Performance of Dye-Sensitized Solar Cells. *Nanoscale* **2015**, *7*, 12010–12017. [CrossRef] [PubMed]
68. Mahmood, A. Recent Research Progress on Quasi-Solid-State Electrolytes for Dye-Sensitized Solar Cells. *J. Energy Chem.* **2015**, *24*, 686–692. [CrossRef]
69. Khanmirzaei, M.H.; Ramesh, S.; Ramesh, K. Hydroxypropyl Cellulose Based Non-Volatile Gel Polymer Electrolytes for Dye-Sensitized Solar Cell Applications Using 1-Methyl-3-Propylimidazolium Iodide Ionic Liquid. *Sci. Rep.* **2015**, *5*. [CrossRef] [PubMed]
70. Zhang, S.; Dong, G.Y.; Lin, B.; Qu, J.; Yuan, N.Y.; Ding, J.N.; Gu, Z. Performance Enhancement of Aqueous Dye-Sensitized Solar Cells via Introduction of a Quasi-Solid-State Electrolyte with an Inverse Opal Structure. *Sol. Energy* **2016**, *127*, 19–27. [CrossRef]
71. Wong, B.C.F.; Ahmad, A.; Hanifah, S.A.; Hassan, N.H. Effects of Ethylene Glycol Dimethacrylate as Cross-Linker in Ionic Liquid Gel Polymer Electrolyte Based on Poly(Glycidyl Methacrylate). *Int. J. Polym. Anal. Charact.* **2016**, *21*, 95–103. [CrossRef]
72. Ri, J.H.; Jin, J.; Xu, J.; Peng, T.; Ryu, K.I. Preparation of Iodine-Free Ionic Liquid Gel Electrolyte Using Polyethylene Oxide (PEO)-Polyethylene Glycol (PEG) and its aApplication in Ti-Foil-based Dye-Sensitized Solar Cells. *Electrochim. Acta* **2016**, *201*, 215–259. [CrossRef]
73. Zhang, Y.; Feng, X.; Li, H.; Chen, Y.; Zhao, J.; Wang, S.; Wang, L.; Wang, B. Photoinduced Postsynthetic Polymerization of a Metal-Organic Framework Toward a Flexible Stand-Alone Membrane. *Angew. Chem. Int. Ed.* **2015**, *54*, 4259–4263. [CrossRef] [PubMed]
74. Medel, S.; Bosch, P. New Fluorescent Hyperbranched Polymeric Sensors as Probes for Monitoring Photopolymerization Reactions. *React. Funct. Polym.* **2015**, *93*, 101–110. [CrossRef]
75. Chan, S.; Bantang, J.P.; Camacho, D. Influence of Nanomaterial Fillers in Biopolymer Electrolyte System for Squaraine-Based Dye-Sensitized Solar Cells. *Int. J. Electrochem. Sci.* **2015**, *10*, 7696–7706.
76. Guo, X.; Tu, D.; Liu, X. Recent Advances in Rylene Diimide Polymer Acceptors for All-Polymer Solar Cells. *J. Energy Chem.* **2015**, *24*, 675–685. [CrossRef]
77. Angulakshmi, N.; Senthil Kumar, R.; Anbu Kulandainathan, M.; Manuel Stephan, A. Composite Polymer Electrolytes Encompassing Metal Organic Frame Works: A New Strategy for All-Solid-State Lithium Batteries. *J. Phys. Chem. C* **2014**, *118*, 24240–24247. [CrossRef]
78. Zhao, J.; Zhang, J.; Hu, P.; Ma, J.; Wang, X.; Yue, L.; Xu, G.; Qin, B.; Liu, Z.; Zhou, X.; *et al.* A Sustainable and Rigid-Flexible Coupling Cellulose-Supported Poly(Propylene Carbonate) Polymer Electrolyte Towards 5 V High Voltage Lithium Batteries. *Electrochim. Acta* **2016**, *188*, 23–30. [CrossRef]
79. Yousif, E.; El-Hiti, G.A.; Hussain, Z.; Altaie, A. Viscoelastic, Spectroscopic and Microscopic Study of the Photo Irradiation Effect on the Stability of PVC in the Presence of Sulfamethoxazole Schiff's Bases. *Polymers* **2015**, *7*, 2190–2204. [CrossRef]
80. Xiang, W.; Huang, W.; Bach, U.; Spiccia, L. Stable High Efficiency Dye-Sensitized Solar Cells Based on a Cobalt Polymer Gel Electrolyte. *Chem. Commun.* **2013**, *49*, 8997–8999. [CrossRef] [PubMed]
81. Bhagavathi Achari, M.; Elumalai, V.; Vlachopoulos, N.; Safdari, M.; Gao, J.; Gardner, J.M.; Kloo, L. A Quasi-Liquid Polymer-Based Cobalt Redox Mediator Electrolyte for Dye-Sensitized Solar Cells. *Phys. Chem. Chem. Phys.* **2013**, *15*, 17419–17425. [CrossRef] [PubMed]

82. Dietlin, C.; Schweizer, S.; Xiao, P.; Zhang, J.; Morlet-Savary, F.; Graff, B.; Fouassier, J.P.; Lalevée, J. Photopolymerization upon LEDs: New Photoinitiating Systems and Strategies. *Polym. Chem.* **2015**, *6*, 3895–3912. [CrossRef]
83. Crivello, J.V.; Reichmanis, E. Photopolymer Materials and Processes for Advanced Technologies. *Chem. Mater.* **2014**, *26*, 533–548. [CrossRef]
84. Tajima, T.; Nishihama, T.; Miyake, S.; Takahashi, N.; Takaguchi, Y. Synthesis and Properties of (Terthiophene)$_4$–Poly(amidoamine)–C60 Pentad. *Bull. Chem. Soc. Jpn.* **2015**, *88*, 736–745. [CrossRef]
85. Wang, P.; Zakeeruddin, S.M.; Comte, P.; Exnar, I.; Grätzel, M. Gelation of Ionic Liquid-Based Electrolytes with Silica Nanoparticles for Quasi-Solid-State Dye-Sensitized Solar Cells. *J. Am. Chem. Soc.* **2003**, *125*, 1166–1167. [CrossRef] [PubMed]
86. Fang, Y.; Zhang, J.; Zhou, X.; Lin, Y.; Fang, S. "Soggy sand" electrolyte based on COOH-functionalized silica nanoparticles for dye-sensitized solar cells. *Electrochem. Commun.* **2012**, *16*, 10–13. [CrossRef]
87. Xu, H.; Zhang, D.; Xu, A.; Wu, F.; Cao, R. Quantum Sized Zinc Oxide Immobilized on Bentonite Clay and Degradation of C.I. Acid Red 35 in Aqueous under Ultraviolet Light. *Int. J. Photoenergy* **2015**, *2015*. [CrossRef]
88. Stergiopoulos, T.; Bidikoudi, M.; Likodimos, V.; Falaras, P. Dye-Sensitized Solar Cells Incorporating Novel Co(II/III) Based-Redox Electrolytes Solidified by Silica Nanoparticles. *J. Mater. Chem.* **2012**, *22*, 24430–24438. [CrossRef]
89. Listorti, A.; O'Regan, B.; Durrant, J.R. Electron Transfer Dynamics in Dye-Sensitized Solar Cells. *Chem. Mater.* **2011**, *23*, 3381–3399. [CrossRef]
90. Yang, W.; Söderberg, M.; Eriksson, A.I.K.; Boschloo, G. Efficient Aqueous Dye-Sensitized Solar Cell Electrolytes Based on a TEMPO/TEMPO$^+$ Redox Couple. *RSC Adv.* **2015**, *5*, 26706–26709. [CrossRef]
91. Lin, R.Y.Y.; Wu, F.L.; Li, C.T.; Chen, P.Y.; Ho, K.C.; Lin, J.T. High-Performance Aqueous/Organic Dye-Sensitized Solar Cells Based on Sensitizers Containing Triethylene Oxide Methyl Ether. *ChemSusChem* **2015**, *8*, 2503–2513. [CrossRef] [PubMed]
92. Cisneros, R.; Beley, M.; Lapicque, F.; Gros, P.C. Hydrophilic Ethylene-Glycol-Based Ruthenium Sensitizers for Aqueous Dye-Sensitized Solar Cells. *Eur. J. Inorg. Chem.* **2016**, *2016*, 33–39. [CrossRef]
93. Fayad, R.; Shoker, T.A.; Ghaddar, T.H. High Photo-Currents with a Zwitterionic Thiocyanate-Free Dye in Aqueous-based Dye Sensitized Solar Cells. *Dalton Trans.* **2016**, *45*, 5622–5628. [CrossRef] [PubMed]
94. Chen, H.C.; Williams, R.M.; Reek, J.N.H.; Brouwer, A.M. Robust Benzo[g, h, i]Perylenetriimide Dye-Sensitized Electrodes in Air-Saturated Aqueous Buffer Solution. *Chem. Eur. J.* **2016**, *22*, 5489–5493. [CrossRef] [PubMed]
95. Amoli, V.; Bhat, S.; Maurya, A.; Banerjee, B.; Bhaumik, A.; Sinha, A.K. Tailored Synthesis of Porous TiO_2 Nanocubes and Nanoparallelepipeds with Exposed {111} Facets and Mesoscopic Void Space: A Superior Candidate for Efficient Dye-Sensitized Solar Cells. *ACS Appl. Mater. Interfaces* **2015**, *7*, 26022–26035. [CrossRef] [PubMed]
96. Heiniger, L.P.; Giordano, F.; Moehl, T.; Grätzel, M. Mesoporous TiO_2 Beads Offer Improved Mass Transport for Cobalt-Based Redox Couples Leading to High Efficiency Dye-Sensitized Solar Cells. *Adv. Energy Mater.* **2014**, *4*. [CrossRef]
97. Xiang, W.; Chen, D.; Caruso, R.A.; Cheng, Y.B.; Bach, U.; Spiccia, L. The Effect of the Scattering Layer in Dye-Sensitized Solar Cells Employing a Cobalt-Based Aqueous Gel Electrolyte. *ChemSusChem* **2015**, *8*, 3704–3711. [CrossRef] [PubMed]
98. Xiang, W.; Huang, F.; Cheng, Y.B.; Bach, U.; Spiccia, L. Aqueous Dye-Sensitized Solar Cell Electrolytes based on the Cobalt(II)/(III) Tris(Bipyridine) Redox Couple. *Energy Environ. Sci.* **2013**, *6*, 121–127. [CrossRef]
99. Kumar, P.; Bansal, V.; Deep, A.; Kim, K.H. Synthesis and Energy Applications of Metal Organic Frameworks. *J. Porous Mater.* **2015**, *22*, 413–424. [CrossRef]
100. Kaur, R.; Kim, K.H.; Paul, A.K.; Deep, A. Recent Advances in the Photovoltaic Applications of Coordination Polymers and Metal Organic Frameworks. *J. Mater. Chem. A* **2016**, *4*, 3991–4002. [CrossRef]
101. Bandyopadhyay, P.; Nandy, P.; Basu, R.; Das, S. Morphology Dependent Change in Photovoltage Generation Using Dye-Cu Doped ZnO Nanoparticle Mixed System. *Energy* **2015**, *89*, 318–323. [CrossRef]
102. Wojnarowicz, J.; Kusnieruk, S.; Chudoba, T.; Gierlotka, S.; Lojkowski, W.; Knoff, W.; Lukasiewicz, M.I.; Witkowski, B.S.; Wolska, A.; Klepka, M.T.; *et al.* Paramagnetism of Cobalt-Doped ZnO Nanoparticles Obtained by Microwave Solvothermal Synthesis. *Beilstein J. Nanotechnol.* **2015**, *6*, 1957–1969. [CrossRef] [PubMed]

103. Xiao, Y.; Cao, M. Dual Hybrid Strategy Towards Achieving High Capacity and Long-Life Lithium Storage of ZnO. *J. Power Sources* **2016**, *305*, 1–9. [CrossRef]
104. Kim, H.B.; Jeong, D.W.; Jang, D.J. Morphology-Tunable Synthesis of ZnO Microstructures Under Microwave Irradiation: Formation Mechanisms and Photocatalytic Activity. *CrystEngComm* **2016**, *18*, 898–906. [CrossRef]
105. Li, H.; Wei, Y.; Zhao, Y.; Zhang, Y.; Yin, F.; Zhang, C.; Bakenov, Z. Simple One-Pot Synthesis of Hexagonal ZnO Nanoplates as Anode Material for Lithium-Ion Batteries. *J. Nanomater.* **2016**, *2016*. [CrossRef]
106. Kim, S.Y.; Kim, B.H. Electrochemical Performance of Activated Carbon Nanofiber with ZnO Nanoparticles for Li-Ion Battery. *Synth. Met.* **2015**, *210*, 386–391. [CrossRef]
107. Minda, I.; Ahmed, E.; Sleziona, V.; Richter, C.; Beu, M.; Falgenhauer, J.; Miura, H.; Schlettwein, D.; Schwoerer, H. Identification of Different Pathways of Electron Injection in Dye-Sensitised Solar Cells of Electrodeposited ZnO using an Indoline Sensitiser. *Phys. Chem. Chem. Phys.* **2016**, *18*, 8938–8944. [CrossRef] [PubMed]
108. Sun, H.; Dong, B.; Su, G.; Gao, R.; Liu, W.; Song, L.; Cao, L. Towards TiO_2 Nanotubes Modified by WO_3 Species: Influence of *ex situ* Crystallization of Precursor on the Photocatalytic Activities of WO_3/TiO_2 Composites. *J. Phys. D: Appl. Phys.* **2015**, *48*. [CrossRef]
109. Shao, G.; Lou, C.; Kang, J.; Zhang, H. Luminescent Down Shifting Effect of Ce-Doped Yttrium Aluminum Garnet Thin Films on Solar Cells. *Appl. Phys. Lett.* **2015**, *107*. [CrossRef]
110. Eronen, A.; Harju, A.; Mutanen, J.; Lajunen, H.; Suvanto, M.; Pakkanen, T.; Kuittinen, M. Micropatterned Luminescent Optical Epoxies. *Opt. Express* **2015**, *23*, 33419–33425. [CrossRef] [PubMed]
111. Jiang, Q.; Rebollar, D.; Gong, J.; Piacentino, E.L.; Zheng, C.; Xu, T. Pseudohalide-Induced Moisture Tolerance in Perovskite $CH_3NH_3Pb(SCN)_2I$ Thin Films. *Angew. Chem. Int. Ed.* **2015**, *54*, 7617–7620. [CrossRef] [PubMed]
112. Zhao, Y.; Zhu, K. Organic-Inorganic Hybrid Lead Halide Perovskites for Optoelectronic and Electronic Applications. *Chem. Soc. Rev.* **2016**, *45*, 655–689. [CrossRef] [PubMed]